THE JOURNAL OF PHYSICAL CHEMISTRY B

Article

pubs.acs.org/JPCB

Sitting at the Edge: How Biomolecules use Hydrophobicity to Tune Their Interactions and Function

Amish J. Patel,[†] Patrick Varilly,[‡,∥] Sumanth N. Jamadagni,[†,⊥] Michael F. Hagan,[§] David Chandler,*[,‡] and Shekhar Garde*[,†]

[†]Howard P. Isermann Department of Chemical & Biological Engineering, and Center for Biotechnology & Interdisciplinary Studies, Rensselaer Polytechnic Institute, Troy, New York 12180, United States

[‡]Department of Chemistry, University of California, Berkeley, California 94720, United States

[§]Martin A. Fisher School of Physics, Brandeis University, Waltham, Massachusetts 02454, United States

Supporting Information

ABSTRACT: Water near extended hydrophobic surfaces is like that at a liquid−vapor interface, where fluctuations in water density are substantially enhanced compared to those in bulk water. Here we use molecular simulations with specialized sampling techniques to show that water density fluctuations are similarly enhanced, even near hydrophobic surfaces of complex biomolecules, situating them at the edge of a dewetting transition. Consequently, water near these surfaces is sensitive to subtle changes in surface conformation, topology, and chemistry, any of which can tip the balance toward or away from the wet state and thus significantly alter biomolecular interactions and function. Our work also resolves the long-standing puzzle of why some biological surfaces dewet and other seemingly similar surfaces do not.

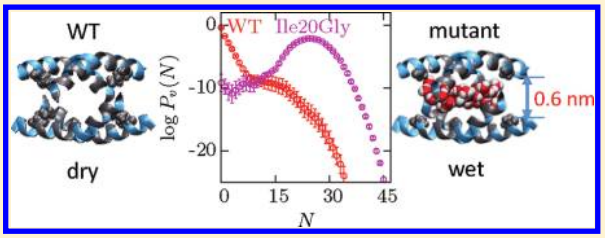

INTRODUCTION: IT IS THE FLUCTUATIONS THAT ARE IMPORTANT

Much of biology happens in aqueous environments, with interfaces of biomolecules being wet.[1,2] Yet, hydrophobically driven assembly leads to contact surfaces that contain little or no water.[3,4] How biomolecules are able to perform the task of removing water from their vicinity is an important open question.[5] Here, building on our earlier theoretical work[6−8] and algorithm development,[9,10] we show explicitly that the answer lies in the proximity of water near hydrophobic surfaces to an underlying phase transition.

Thermodynamically, bulk water at ambient conditions is already close to the liquid−vapor phase boundary.[11,12] Near a weakly interacting hydrophobic surface, water molecules are pulled toward the bulk (and away from the surface), where they can interact with other waters much more strongly.[6,13] Hence, compared to that in the bulk, liquid water near hydrophobic surfaces is further destabilized with respect to its vapor, pushing it toward the edge of a dewetting transition. Indeed, idealized repulsive hydrophobic surfaces nucleate a soft liquid−vapor like interface.[6,9,11,14,15] However, weak attractive van der Waals forces exerted by a realistic hydrophobic surface are sufficient to pull the soft interface adjacent to the surface, rewetting it[16−23] and masking the proximity to the underlying dewetting transition. Crucially, this underlying transition is thus manifest not in the mean water density near the surface but instead in two inter-related phenomena: the significant enhancement of fluctuations away from the mean[9] and an enhanced susceptibility of water density to perturbations.[11,17,22,24]

Here we employ specialized sampling techniques[9,10] to measure water density fluctuations near two complex biomolecules previously studied in the context of dewetting.[2,25] We illustrate the enhancement of water density fluctuations near a sufficiently hydrophobic patch on the biomolecular surface and demonstrate how the concomitant sensitivity of water density to perturbations near such surfaces can be exploited through small perturbations, including subtle conformational changes. Our results explain why gaps between two hydrophobic protein surfaces can be wet in one protein system[2] and dry in another.[25] The two systems are close to, but on either side of, the dewetting transition.

METHODS

We study three classes of systems with water next to a hydrophobic surface, described in detail below. These are: (1) self-assembled monolayers (SAMs) of alkyl chains with headgroup chemistries that render the SAM−water interface either hydrophobic ($-CH_3$) or hydrophilic ($-OH$); (2) the surface of domain I of a single subunit of the BphC enzyme, both when isolated and when in proximity to domain II of the subunit; and (3) the surface of a melittin dimer, both when isolated and in proximity to another melittin dimer. In each system, we pick a probe volume v close to the surface of interest and calculate the probability $P_v(N)$ of observing N

Received: November 8, 2011
Revised: December 30, 2011
Published: January 11, 2012

   dx.doi.org/10.1021/jp2107523 | J. Phys. Chem. B 2012, 116, 2498−2503

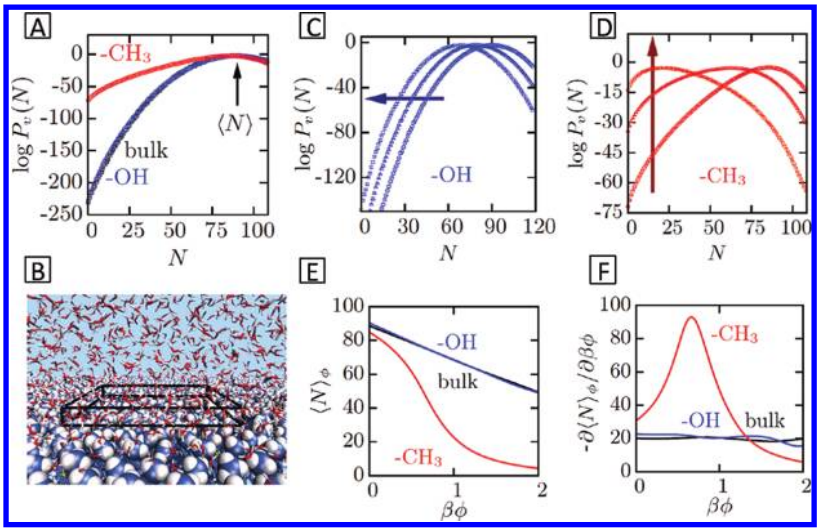

Figure 1. Water density fluctuations and their response to perturbations near hydrophobic and hydrophilic interfaces. (A) $P_\nu(N)$ for a 3 × 3 × 0.3 nm^3 cuboid ν in bulk water and at the interface of hydrophobic ($-CH_3$) and hydrophilic (−OH) self-assembled monolayer (SAM) surfaces. (B) A close-up view of the $-CH_3$ SAM−water interface. Water (sticks, oxygen in red, hydrogen in white), $-CH_3$ head groups (spacefill, carbon in purple, hydrogen in white), and the volume ν (black wireframe) are shown. (C) and (D) $P_\nu(N)$ distributions near the −OH and the $-CH_3$ SAMs, respectively, in the presence of an unfavorable linear potential, ϕN, for $\phi = 0$ (no perturbation), $\phi = 0.5k_BT$, and $\phi = 1k_BT$. The arrow points in the direction of increasing ϕ. (E) The response of the average number of water molecules in the volume ν, $\langle N\rangle_\phi$, to the external potential ϕ, and (F) the corresponding susceptibility, $-\partial\langle N\rangle_\phi/\partial\beta\phi$, show signatures of a nanoscopic phase transition near the $-CH_3$ surface. Error bars calculated using six separate simulation blocks are smaller than the symbols used.

waters in ν, using the indirect umbrella sampling (INDUS) method.[9,10] The full probability distribution $P_\nu(N)$ yields insightful information about the sensitivity of the number of waters in ν to external perturbations, an insight that the mean number of waters in ν alone fails to provide.[9]

We explore these systems with simulations, performed using the GROMACS[26] molecular dynamics package, which was suitably modified to allow for importance sampling using INDUS. All calculations were done in the NVT ensemble (T = 300 K), with a buffering vapor−liquid interface.[9,27] Electrostatic interactions were calculated using the particle-mesh Ewald algorithm.[28] For the protein studies, the net charge of the proteins was neutralized by adding the requisite numbers of Na^+ or Cl^- ions.

SAM Surfaces. We consider SAM surfaces that have been described in detail previously.[20,29] For ν, we use a 3 × 3 × 0.3 nm^3 cuboid, which we place either in the region of bulk water or immediately adjacent to the SAM (Figure 1A). To explore how external perturbations affect the stability of water in ν, we use an idealized linear coupling ϕN between a tunable external field ϕ and the number of waters N in ν.

BphC Domains. To explore whether the principles governing the dewetting of the model SAM surfaces extend to the topologically and chemically complex surfaces of biomolecules, we study the stability of water around the two domains of a BphC subunit, whose association is mediated by large hydrophobic patches between the two domains.[2] Domain I of BphC, parametrized using the AMBER-94 force field, was solvated in about 7500 TIP3P water molecules, whereas simulations of both domains I and II contained about 9500 waters. To study the region between the two domains, domain II was translated along the vector joining the center of masses of the two domains by 0.4, 0.6, and 0.8 nm from the crystal structure (PDB: 1DHY). To prevent diffusion of the protein while still allowing some thermal motion of the side chains, 21 atoms in each domain of BphC were position-restrained harmonically. Bonds involving hydrogen atoms were constrained using the SHAKE algorithm,[30] and temperature was maintained at 300 K using the Berendsen thermostat.[31] To explore how perturbations affect the stability of water near BphC's hydrophobic surfaces, we perform an additional set of calculations with all partial charges in the protein turned off, which artificially renders its surfaces to be more hydrophobic.

For ν, we use volumes in the hydration shell of BphC that complement the shape of the protein surface (Figure 2A). Specifically, using a cubic grid with a spacing of 0.3 nm laid over the simulation box, we choose a sufficiently large, contiguous patch of about 40 grid cells, such that no cell contained any protein heavy atoms. Additionally, to probe a patch on the protein surface with a prevalence of hydrophobic residues, each cell constituting ν was required to be within 0.4 nm of at least one of the designated hydrophobic amino acids (Val, Leu, Ile, and Phe) and at least 0.8 nm away from the designated hydrophilic amino acids (Lys, Arg, Asp, and Glu). The probe volume near a hydrophilic patch was chosen similarly (Figure 2A). Finally, to study the gap between the two domains, the cells were chosen with the additional constraint that they had to be in the interdomain region (Figure 2, panels D and E). Note that the procedure described here for choosing ν is only effective if the overall position and orientation of the protein is constrained. These constraints ensure that the region of space corresponding to the first hydration shell of the protein does not change throughout the simulation and also make it possible to fix the distance between the protein domains.

Melittin Dimers. We also characterized the fluctuations of water around the hydrophobic surfaces of melittin dimers and tetramers, parametrized with the AMBER-99sb force field and solvated in about 5000 SPC/E water molecules. To study the region between the two dimers, one of the dimers from the tetramer crystal structure (PDB: 2MLT) was successively translated along the dimer−dimer vector by 0.6, 0.7, 0.8, and 0.9 nm. The backbone atoms of the dimers were constrained

dx.doi.org/10.1021/jp2107523 | J. Phys. Chem. B 2012, 116, 2498−2503

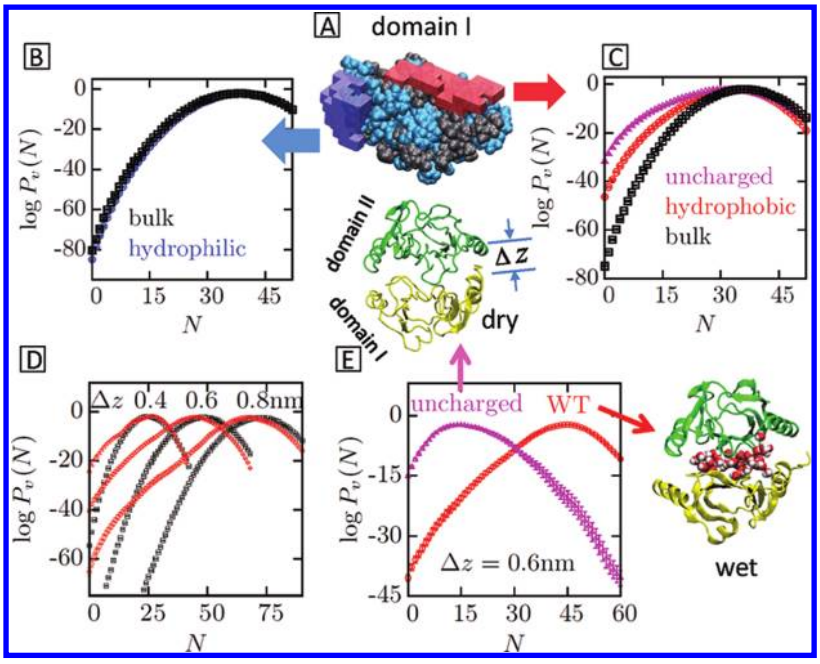

Figure 2. Density fluctuations and the corresponding wetting and drying of BphC domains. (A) Snapshot of domain I (residues 1−135) of a BphC subunit (PDB: 1DHY) showing hydrophobic (gray) and hydrophilic (blue) regions. Also shown are the two separate 0.3 nm thick observation volumes complementing the protein surface near a hydrophobic (red) and a hydrophilic (blue) patch. (B) $P_\nu(N)$ near the hydrophilic patch is similar to that in bulk water. (C) $P_\nu(N)$ near the hydrophobic patch displays enhanced low-N fluctuations. When electrostatic interactions between the protein and the water are turned off, the fluctuations are enhanced further, indicating that the protein surface becomes more hydrophobic. (D) $P_\nu(N)$ distributions in an observation volume sandwiched between the two domains of the BphC subunit for different interdomain separations, Δz = 0.8, 0.6, and 0.4 nm (red). Distributions in similar volumes in bulk water are shown for comparison (black). (E) $P_\nu(N)$ distributions in the interdomain region for Δz = 0.6 nm, for proteins with charges on [same as in (D)] and off. Error bars were calculated using six separate simulation blocks.

harmonically. Bonds within melittin were constrained using the P-LINCS algorithm,[32] while those in the water were constrained with the SETTLE algorithm.[33] Temperature was maintained at 300 K using the canonical velocity rescaling thermostat of Bussi and co-workers.[34]

To select the probe volume ν for a given separation between the dimers, the convex hull of the C^α positions of residues 8 and 20 of each monomer (8 points in total) was calculated, and a 0.1 nm resolution grid was placed in the system. Grid cells whose centers were both inside the convex hull and outside the van der Waals radius of each protein heavy atom were selected to be part of the probe volume. We considered both wild-type melittin and the mutants resulting from six different point mutations studied previously.[25] The probe volume was slightly different for each mutant. To select a probe volume near an isolated dimer, the convex hull for a separation of 0.4 nm between the wild-type dimers was computed. Grid cells in this convex hull that do not overlap with protein heavy atoms of the dimer of interest constitute the probe volume of that dimer. The same probe volume was used for all mutant dimers, allowing a direct comparison of density fluctuations near them.

RESULTS

Water Density Fluctuations and the Dewetting Transition near Self-Assembled Monolayers. As a preliminary to studying biomolecular surfaces, we illustrate that water density fluctuations provide a clear signature of hydrophobicity. To this end, we calculated $P_\nu(N)$ in the SAM system (Figure 1A), with ν in the bulk, as well as next to the $-CH_3$ or $-OH$ SAMs. The average number, $\langle N\rangle$, of water molecules in ν, reflected in the peak of $P_\nu(N)$, is similar in all three cases, indicating that both the SAMs are wet. The density fluctuations in bulk water and at the hydrophilic $-OH$ SAM are also similar and approximately Gaussian (parabolic on a log scale), as expected.[9] However, fluctuations near the hydrophobic $-CH_3$ SAM are different, with $P_\nu(N)$ enhanced significantly for low N-values.[9] Because the differences in the distributions at low N correspond to fluctuations that are extremely rare, they do not affect the average equilibrium behavior. However, these rare fluctuations play an important role in the presence of a perturbation. For example, the response of water near the $-CH_3$ and $-OH$ surfaces to the unfavorable linear potential, ϕN, is very different. Near the $-OH$ surface, increasing ϕ shifts the distribution to the left (Figure 1C) and lowers the mean density of water, $\langle N\rangle_\phi$, gradually (Figure 1E). In contrast, near the $-CH_3$ surface, even small ϕ-values, of the order of the thermal energy (k_BT per water), are sufficient to dramatically alter the distribution, with low-N fluctuations being enhanced so much that they become the most probable ones (Figure 1D). As a result, even a small unfavorable perturbation is able to dry the hydrophobic $-CH_3$ surface, and $\langle N\rangle_\phi$ decreases precipitously (Figure 1E). Correspondingly, the sensitivity of water density to perturbations, quantified by the susceptibility, $-\partial\langle N\rangle_\phi/\partial\phi$, displays a peak near the hydrophobic surface (Figure 1F), a known feature of phase transitions. Thus, the remarkable sensitivity of water density to perturbations is directly connected to the enhanced low-N fluctuations, with both observations resulting from the proximity of water to an underlying dewetting transition.[6,9,11,17]

Biomolecular Surfaces Can Display Enhanced Fluctuations Too. In contrast to the flat, uniform SAM surfaces, the

dx.doi.org/10.1021/jp2107523 | J. Phys. Chem. B 2012, 116, 2498−2503

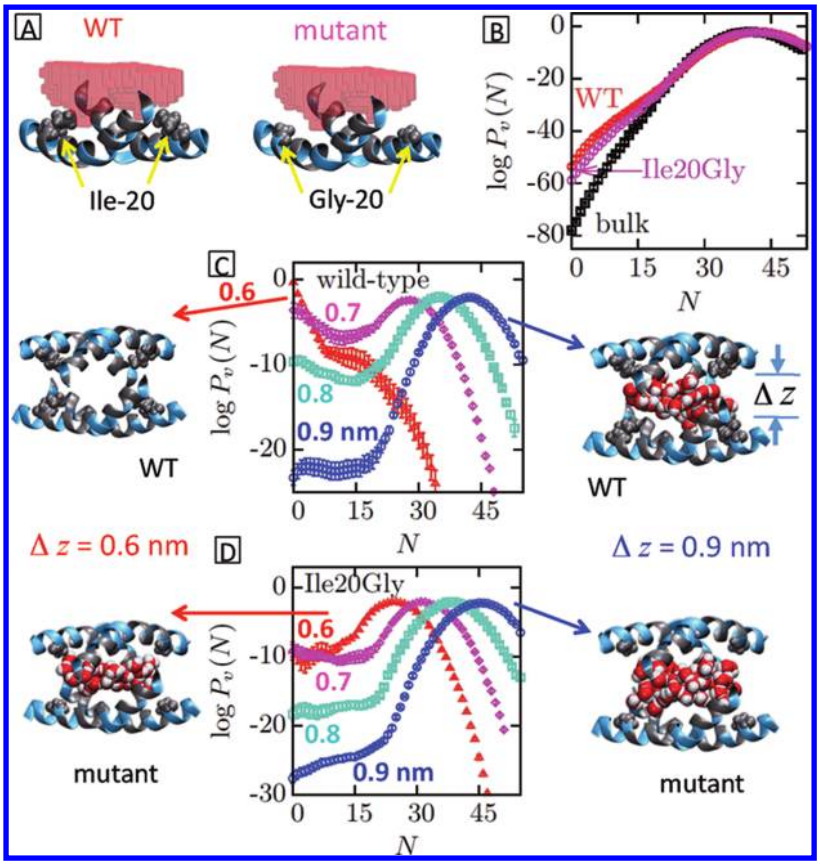

Figure 3. Melittin dimer association. (A) Snapshot highlighting the observation volume near the hydrophobic surface of the wild-type melittin (WT) dimer (PDB: 2MLT) and the Ile20Gly mutant dimer. The mutation is shown in spacefill representation. (B) $P_v(N)$ distributions in the observation volumes shown in (A) and in a similar volume in bulk water. (C) $P_v(N)$ distributions in the observation volume between two WT melittin dimers for dimer−dimer separations, Δz, of 0.9 (blue), 0.8 (cyan), 0.7 (magenta), and 0.6 nm (red) indicate a dewetting transition for $\Delta z < 0.7$ nm. Representative equilibrium snapshots of the tetramer at $\Delta z = 0.6$ (dry) and 0.9 nm (wet) are shown. Water molecules in the observation volumes are shown in spacefill representation, and the remaining waters have been omitted for clarity. (D) Same as in (C) for the Ile20Gly mutants, where no dewetting is observed. Error bars were calculated using six separate simulation blocks.

surfaces of the BphC domains are rugged (Figure 2A), so the probe volume v is not cuboidal but instead has an irregular shape that envelopes the first solvation shell of water near the protein. Figure 1B shows that $P_v(N)$ near a hydrophilic patch on the domain I surface is bulk-like, similar to that near the −OH SAM. In contrast, despite the presence of a highly polar backbone and possible interactions with charged side chains and counterions, $P_v(N)$ near a hydrophobic patch on the isolated domain I surface shows enhanced low-N fluctuations (Figure 2C), similar to those seen near the $-CH_3$ SAM.

BphC Surfaces: On the Wet Side of the Dewetting Transition. To investigate how water near the hydrophobic patch responds to realistic perturbations, we place domain II near domain I at different separations, Δz, and calculate $P_v(N)$ in the space between the two domains. As the domains are brought closer, the likelihood of drying, given by $P_v(N) \approx 0$, increases (Figure 1D), but the interdomain region remains wet. Even at $\Delta z = 0.4$ nm, where only a single layer of water can be accommodated between the domains, the average value of N, given by the peak of $P_v(N)$, is high, consistent with the findings of ref 2. This might seem surprising given the prevalence of hydrophobic residues on the protein surfaces surrounding the interdomain region. However, $P_v(N)$ distributions at all Δz display enhanced low-N fluctuations, suggesting that water is at the edge of a dewetting transition, albeit on the wet side.

Tipping the Balance in BphC. If this is indeed the case, a sufficient additional perturbation should be able to push it over the edge and trigger dewetting. To test this, and motivated by Zhou et al.,[2] we turned off the partial charges on the protein, a perturbation that should disfavor the presence of water. As a result, the hydrophobicity of the patch on the isolated domain I surface is enhanced, as reflected in the enhanced fluctuations in Figure 2C. The effect of this perturbation on water in the interdomain region is dramatic: an essentially dry state is now preferred even at a distance of 0.6 nm between the domain surfaces (Figure 2E). By explicitly examining the configurations of water in v under these conditions, it is clear that the approximately 15 waters that, on average, remain inside the probe volume v are confined to its edges, not distributed uniformly within v. Hence, the fact that $P_v(N)$ is not peaked at $N = 0$ but at $N \approx 15$ merely reflects the crudeness with which we have identified the interdomain cavity that dewets and is not indicative of partial dewetting.

Melittin Surfaces: On the Dry Side of the Dewetting Transition. In contrast to the assembly of BphC domains, that of melittin dimers represents a system which sits on the dry side of the dewetting transition.[25] We calculated $P_v(N)$ near the putative hydrophobic face of an isolated dimer surface (Figure 3A), which indeed displays enhanced fluctuations (Figure 3B), as expected. Correspondingly, when the system is perturbed by placing a second wild-type dimer nearby, a drying transition in

dx.doi.org/10.1021/jp2107523 | J. Phys. Chem. B 2012, 116, 2498−2503

the space between the dimers is clearly seen in the $P_v(N)$ distributions in Figure 3C. For Δz = 0.9 nm, the average value of N, given by peak of $P_v(N)$, is high, implying a wet state. On the other hand, for Δz = 0.6 nm, the space between the dimers is dry. Interestingly, for intermediate values of Δz (0.7 and 0.8 nm), the $P_v(N)$ distributions show bimodal behavior, indicating the presence of a desolvation barrier separating the wet and dry states (repectively, high and low N). Barriers along this simple order parameter, N, can play an important role in governing the kinetics of dimer−dimer assembly.[35,36]

Tipping the Balance in Melittin. Although a drying transition is observed for the wild-type melittin dimers, once again, it is extremely sensitive to small perturbations, such as point mutations, as noted by Berne and co-workers.[25] We calculated $P_v(N)$ distributions near six isolated melittin dimer mutants, which all show enhanced fluctuations, with subtle differences between them (see Supporting Information). To highlight the effect of a perturbation on the drying transition in melittin, we focus on one of the mutants, Ile20Gly (Figure 3A). There are only subtle differences in the $P_v(N)$ distributions near the isolated wild-type and the mutant dimer (Figure 3B). However, they translate into dramatic differences in confinement, where the system is poised at the edge of a dewetting transition. Specifically, the Ile20Gly mutant no longer displays a drying transition, as the average value of N remains high even at the smallest Δz (Figure 3D). Thus, the data in Figures 2 and 3 underscore that both BphC and melittin sit at the edge of a wetting−dewetting transition, one on the wet and the other on the dry side, and each can be pushed to the other side by a small perturbation. This proximity to the phase transition (and not the presence of a dewetted state) is the signature of hydrophobic hydration. Further, as the mean water density changes precipitously near the dewetting transition (Figure 1E), it is a poor indicator of the proximity to the transition, which is instead revealed by water density fluctuations.

Implications on Biomolecular Interactions and Function. To enable regulation, biological systems are generically thought to position themselves near phase transitions.[37] Our application of specialized techniques that measure rare fluctuations[9,10] allowed us to highlight that water near hydrophobic surfaces of biomolecules is similarly situated at the edge of a dewetting transition and is sensitive to small perturbations. This sensitivity provides biomolecules with the powerful ability to tune their interactions and function by manipulating the local context, for example, by confining water between them or by changing their shape or chemistry.[23,38−41] Given that desolvation is a component of the reaction coordinate for hydrophobically driven assembly,[27,42] manipulating wetting−dewetting may appreciably influence the kinetics of assembly. Dewetting transitions are also central in the function of some ion channels (such as the mechano-sensitive channel, MscS), where a 10−20 Å long interior hydrophobic wall of the channel provides gating by the "vapor lock" mechanism: a wet channel conducts ions rapidly, whereas a small conformational change can dry the channel and stop ion conduction completely.[43−45] Dewetting can also be induced by manipulating solution conditions, such as temperature, pressure, pH, and cosolvent or solute concentration.[24,46−48] Finally, the sensitivity of nanoscale dewetting transitions is also responsible for the spontaneous filling and emptying of hydrophobic nanotubes[49]and can be harnessed in various other nonbiological settings, ranging from switches in nanofluidic devices and networks[46] to aqueous solution based catalysis in hydrophobic zeolites.[50]

■ ASSOCIATED CONTENT

Supporting Information

A figure showing water density fluctuations for six mutant melittin dimers and tetramers. This material is available free of charge via the Internet at http://pubs.acs.org.

■ AUTHOR INFORMATION

Corresponding Author

*E-mail: chandler@berkeley.edu; gardes@rpi.edu.

Present Addresses

[‖]Department of Chemistry, University of Cambridge, Lensfield Road, CB2 1EW, United Kingdom.

[⊥]Procter and Gamble Company, Beckett Ridge Technical Center, West Chester, OH 45069, USA.

■ ACKNOWLEDGMENTS

S.G. acknowledges partial financial support from NSF (CBET-0967937) and NSEC (DMR-0642573) grants. While carrying out this research, PV was supported by NIH (R01-GM078102-04) grant, and DC received partial support from the U.S. Department of Energy (DOE) (Contract No. DE-AC02-05CH11231). MFH acknowledges financial support from NIH (NIAID R01-AI080791) grant. We also thank Hari Acharya, Ravi Kane, and Kafui Tay for helpful discussions.

■ REFERENCES

(1) Cheng, Y.; Rossky, P. *Nature* **1998**, *392*, 696−699.
(2) Zhou, R.; Huang, X.; Margulis, C. J.; Berne, B. J. *Science* **2004**, *305*, 1605−1609.
(3) Larsen, T. A.; Olson, A. J.; Goodsell, D. S. *Structure* **1998**, *6*, 421−427.
(4) Rodier, F.; Bahadur, R. P.; Chakrabarti, P.; Janin, J. *Proteins: Struct., Funct., Bioinf.* **2005**, *60*, 36−45.
(5) Krone, M. G.; Hua, L.; Soto, P.; Zhou, R.; Berne, B. J.; Shea, J.-E. *J. Am. Chem. Soc.* **2008**, *130*, 11066−11072.
(6) Lum, K.; Chandler, D.; Weeks, J. D. *J. Phys. Chem. B* **1999**, *103*, 4570−4577.
(7) Huang, D. M.; Chandler, D. *Phys. Rev. E* **2000**, *61*, 1501−1506.
(8) Varilly, P.; Patel, A. J.; Chandler, D. *J. Chem. Phys.* **2011**, *134*, 074109.
(9) Patel, A. J.; Varilly, P.; Chandler, D. *J. Phys. Chem. B* **2010**, *114*, 1632−1637.
(10) Patel, A. J.; Varilly, P.; Chandler, D.; Garde, S. *J. Stat. Phys.* **2011**, *145*, 265−275.
(11) Chandler, D. *Nature* **2005**, *437*, 640−647.
(12) Cerdeirina, C. A.; Debenedetti, P. G.; Rossky, P. J.; Giovambattista, N. *J. Phys. Chem. Lett.* **2011**, *2*, 1000−1003.
(13) Weeks, J. D. *Annu. Rev. Phys. Chem.* **2002**, *53*, 533−562.
(14) Stillinger, F. H. *J. Solution Chem.* **1973**, *2*, 141−158.
(15) Mittal, J.; Hummer, G. *Proc. Natl. Acad. Sci. U.S.A.* **2008**, *105*, 20130−20135.
(16) Wallqvist, A.; Gallicchio, E.; Levy, R. M. *J. Phys. Chem. B* **2001**, *105*, 6745−6753.
(17) Huang, D. M.; Chandler, D. *J. Phys. Chem. B* **2002**, *106*, 2047−2053.
(18) Lee, C.-Y.; McCammon, J. A.; Rossky, P. J. *J. Chem. Phys.* **1984**, *80*, 4448−4455.
(19) Ashbaugh, H. S.; Paulaitis, M. E. *J. Am. Chem. Soc.* **2001**, *123*, 10721−10728.
(20) Godawat, R.; Jamadagni, S. N.; Garde, S. *Proc. Natl. Acad. Sci. U.S.A.* **2009**, *106*, 15119−15124.

(21) Mezger, M.; Reichert, H.; Schoder, S.; Okasinski, J.; Schroder, H.; Dosch, H.; Palms, D.; Ralston, J.; Honkimaki, V. *Proc. Natl. Acad. Sci. U.S.A.* **2006**, *103*, 18401−18404.
(22) Sarupria, S.; Garde, S. *Phys. Rev. Lett.* **2009**, *103*, 037803.
(23) Acharya, H.; Vembanur, S.; Jamadagni, S. N.; Garde, S. *Faraday Discuss.* **2010**, *146*, 353−365.
(24) Giovambattista, N.; Rossky, P. J.; Debenedetti, P. G. *Phys. Rev. E* **2006**, *73*, 041604.
(25) Liu, P.; Huang, X.; Zhou, R.; Berne, B. J. *Nature* **2005**, *437*, 159−162.
(26) Hess, B.; Kutzner, C.; van der Spoel, D.; Lindahl, E. *J. Chem. Theory Comput.* **2008**, *4*, 435.
(27) Miller, T.; Vanden-Eijnden, E.; Chandler, D. *Proc. Natl. Acad. Sci. U.S.A.* **2007**, *104*, 14559−14564.
(28) Essmann, U.; Perera, L.; Berkowitz, M. L.; Darden, T.; Lee, H.; Pedersen, L. G. *J. Chem. Phys.* **1995**, *103*, 8577−8593.
(29) Patel, A. J.; Varilly, P.; Jamadagni, S. N.; Acharya, H.; Garde, S.; Chandler, D. *Proc. Natl. Acad. Sci. U.S.A.* **2011**, *108*, 17678−17683.
(30) Ryckaert, J.-P.; Ciccotti, G.; Berendsen, H. J. C. *J. Comput. Phys.* **1977**, *23*, 327−341.
(31) Berendsen, H. J. C.; Postma, J. P. M; Vangunsteren, W. F.; Dinola, A.; Haak, J. R. *J. Chem. Phys.* **1984**, *81*, 3684−3690.
(32) Hess, B. *J. Chem. Theory Comput.* **2008**, *4*, 116−122.
(33) Miyamoto, S.; Kollman, P. A. *J. Comput. Chem.* **1992**, *13*, 952−962.
(34) Bussi, G.; Donadio, D.; Parrinello, M. *J. Chem. Phys.* **2007**, *126*, 014101.
(35) Leung, K.; Luzar, A.; Bratko, D. *Phys. Rev. Lett.* **2003**, *90*, 065502.
(36) Huang, X.; Margulis, C. J.; Berne, B. J. *Proc. Natl. Acad. Sci. U.S.A.* **2003**, *100*, 11953−11958.
(37) Mora, T.; Bialek, W. *J. Stat. Phys.* **2011**, *143*, 1−35.
(38) Beckstein, O.; Sansom, M. S. P. *Phys. Biol.* **2004**, *1*, 42.
(39) Giovambattista, N.; Lopez, C. F.; Rossky, P. J.; Debenedetti, P. G. *Proc. Natl. Acad. Sci. U.S.A.* **2008**, *105*, 2274−2279.
(40) Hua, L.; Zangi, R.; Berne, B. J. *J. Phys. Chem. C* **2009**, *113*, 5244−5253.
(41) Mittal, J.; Hummer, G. *Faraday Discuss.* **2010**, *146*, 341−352.
(42) ten Wolde, P. R.; Chandler, D. *Proc. Natl. Acad. Sci. U.S.A.* **2002**, *99*, 6539−6543.
(43) Anishkin, A.; Sukharev, S. *Biophys. J.* **2004**, *86*, 2883−2895.
(44) Chakrabarti, N.; Neale, C.; Payandeh, J.; Pai, E. F.; Pomès, R. *Biophys. J.* **2010**, *98*, 784−792.
(45) Zhu, F.; Hummer, G. *Proc. Natl. Acad. Sci. U.S.A.* **2010**, *107*, 19814−19819.
(46) Rasaiah, J. C.; Garde, S.; Hummer, G. *Annu. Rev. Phys. Chem.* **2008**, *59*, 713−740.
(47) Giovambattista, N.; Rossky, P. J.; Debenedetti, P. G. *J. Phys. Chem. B* **2009**, *113*, 13723−13734.
(48) England, J. L.; Pande, V. S.; Haran, G. *J. Am. Chem. Soc.* **2008**, *130*, 11854−11855.
(49) Hummer, G.; Rasaiah, J. C.; Noworyta, J. P. *Nature* **2001**, *414*, 188−190.
(50) Moliner, M.; Roman-Leshkov, Y.; Davis, M. E. *Proc. Natl. Acad. Sci. U.S.A.* **2010**, *107*, 6164.